Chapter 6

Results and interpretations

In this chapter, the results obtained have been presented first; which include- the decreasing brightness of the light scattered by dust as a function of optocentric distance, the intensity images using some enhancement techniques, the linear polarization in terms of aperture polarization and polarization maps. After that, the results have been interpreted and based on those discussions, some conclusion have been drawn.

6.1 Background discussion of present work

In complement to photometric and spectroscopic observations, linear polarization studies give some indications for the optical and physical properties of dust grains ejected by comets when they approach the Sun. Previous works by the polarimetric imaging method have revealed that different regions inside coma show differences in polarization suggesting differences in physical properties of the dust particles. Jets, fan-like structures usually show a higher polarization than the background coma. In some comets, regions close to the nucleus are marked by a smaller positive polarization value at phase angles larger than the inversion angle and a deeper negative polarization at phase angles smaller than the inversion angle. Some of those variations are not yet completely interpreted. (e.g. [Dollfus and Suchail, 1987], [Sen et al., 1990], [Renard et al., 1992], [Hadamcik and Levasseur-Regourd, 2003c], [Hadamcik and Levasseur-Regourd, 2003b]). To

contribute towards better understanding of these polarimetric results, some Indian and French astronomers in the joint campaign under CEFIPRA (Indo French Centre for the Promotion of Advanced Research) funded project (No. 4507-1), in which the author worked as a research fellow, observed and studied comets appearing close to Earth. (e.g. [Hadamcik et al., 2014], [Roy Choudhury et al., 2014], [Roy Choudhury et al., 2015]). In the following sections, the polarimetric results of the concerned comets (C/2009 P1 (Garradd), 78P/Gehrels, C/2007 N3 (Lulin), C/2011 L4 (PANSTARRS), 290P/Jager) observed and studied under the said project will be discussed.

Prior to the sanctioning of CEFIPRA, No. 4507-1, the above mentioned Indian and French astronomers jointly observed some other comets such as 67P/Chruryumov-Gerasimenko, 103P/Hartley 2. Comet 67P/Churyumov-Gerasimenko was one of the targets of the Rosetta spacecraft in 2014-2015. The long-time polarization evolution revealed emission of large particles before perihelion and fluffy faster particles just after perihelion. These dust emissions seemed to be correlated with the nucleus rotation and illumination [Hadamcik et al., 2010]. Comet 103PHartley 2 observations included the period of fly-bye by the deep impact spacecraft during the EPOXI mission. The high polarization regions correspond to the jets as emphasized by the nucleus rotation [Hadamcik et al., 2013].

6.2 The results obtained

For the concerned comets, azimuthally integrated radial profiles of intensity and profiles of decrease in intensity along solar and anti-solar directions are presented first in this section. Coma morphologies (obtained from intensity images) followed by aperture linear polarization and polarization maps are presented subsequently. The variation in polarization values is studied with increase in aperture and the polarization maps are obtained to detect variation in polarization in different regions inside the coma. The variations in polarization can declare any decisive relation with different structures noticed in coma morphologies.

6.2.1 Intensity images:

Intensity images are obtained by adding two mutually orthogonal polarized components, keeping in notice that their centers are precisely matched. For IGO, the components are the ordinary and extraordinary portions of an image for each HWP position and that for OHP are either (I_0, I_{90}) or (I_{45}, I_{135}). The successive intensity images thus obtained have to be similar and so, all the intensity images obtained for a particular set are added to build the final intensity images.

Intensity radial profile

Decrease in intensity as a function of optocentric distance is measured for all the comets from the intensity images. To do that, the total intensity value is calculated in increasing apertures for each radial distance from the optocenter. From the aperture intensity values, the intensity in one pixel thickness annulus is computed out, and then divided by the number of pixels in that annulus. The log of the intensity values as a function of log of radial distance (in km) from optocenter is called azimuthally averaged radial intensity log-log profile (profiles in Fig. (6.1), (6.2)). For an isotropic coma, the slope of decrease would be nominal (-1). At large distances from the optocenter, the (-1) slope indicates that all the ejected dust moves on an average progressively away from the nucleus and the sky background has been subtracted properly.

Gehrels:

Fig. (6.1) compares the azimuthally integrated radial profiles with decrease in intensity along the solar and anti-solar directions as a function of the optocentric distance in log-log scale for October, 2011; January and February, 2012 respectively. The azimuthally integrated profiles are first considered. For October, the slope is found to be about -1 for radial distance larger than 5400 km from optocenter. It is below -0.7 within the radial distance 2400 km. Between 2400 and 5400 km, there is a more pronounced decrease with slope -1.38. For January, the slope around -1 (which is $\sim$ -1.03) is detected in a region from 11000 km to 19500 km. Further away, a faint star tracks in the field of view. Between 2440 and 4880 km the slope is found to be -1.38 and that between 5000 km and 11000 km is -1.33.

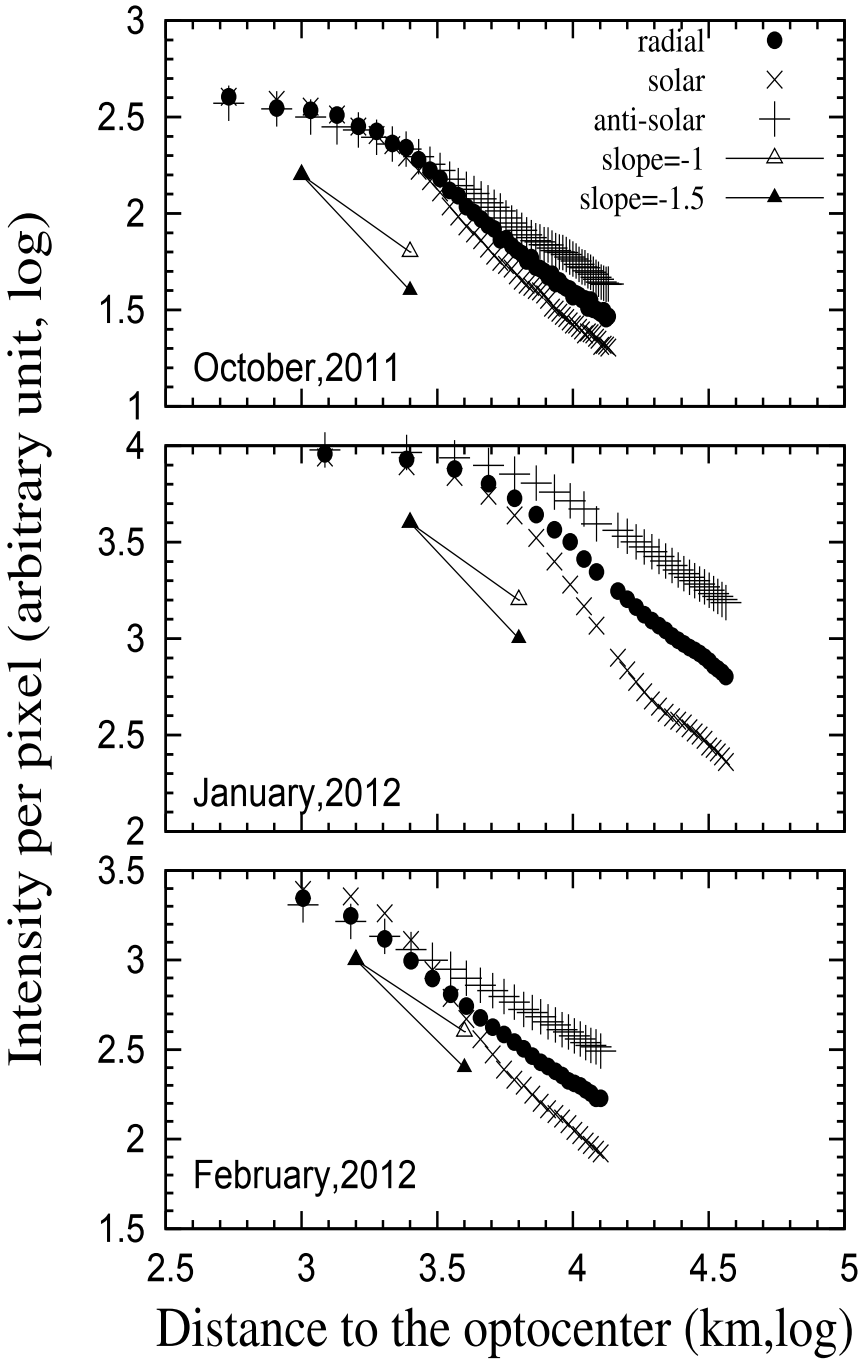

Figure 6.1: Radial, solar, anti-solar profiles of intensity for Gehrels.
The azimuthally integrated radial profiles of intensity, along with the profiles of decrease in intensity along solar and anti-solar directions have been obtained as a function of optocentric distance in log-log scale for the three periods of observations. Fits with -1 and -1.5 slope have also been shown.

For February, the slope is around -1 for optocentric distance larger than 8000 km. From 2500 to 5000 km, the slope is about -1.23 and between 5000 and 8000 km it is about -1.08.

For October observation, it is found that the slope along anti-solar is slightly smaller than -1 (which is $\sim$ -0.95) after 2400 km. Prior to that, the slope is -0.55 from 1600 km to 2400 km. For January and February observation also, the slope along anti-solar is slightly smaller than -1 (which is $\sim$ -0.90) at large distances from optocenter. During January, the slope is -0.30 between 2440 km and 7320 km and -0.92 between 7320 km and 45000 km. In February, it is -0.71 between 1500 km and 3000 km, -0.79 between 3000 km and 7000 km, -0.85 between 7000 km and 12500 km. But along the solar direction, values of slope are quite higher than -1. During October, the slope increases stiffly progressively from -0.87 between 1350 km and 2400 km to -1.56 between 2400 km and 5400 km. During January and February also, the slope along solar profile is found to be greater than -1. For February, it is -0.63 from 2440 km to 6100 km, -1.99 from 6100 km to 18300 km and -1.13 from 20000 km to 36600 km. For February, the slope is -0.74 between 1500 km to 2000 km, -1.55 from 2000 to 2500 km, -2.12 from 2500 km to 5000 km, -1.8 from 5000 km to 10000 km.

Lulin: For Lulin, the slope of decrease on the radial profile is found to be about -1 for radial distance larger than 1080 km from the optocenter. It is around -1.16 between 540-1080 km and -0.9 within the radial distance 540 km. The slope along anti-solar direction is -1.06 between 1080-1750 km and that between 400-1080 km is about -1.2. Along solar direction, the slope is -1.2 between 540-1080 km and -1 after 1080 km.

C/2011 L4: In case of C/2011 L4, for optocentric distance larger than 4700 km, the slope of radial profile is around -1.17. From 1170 to 4700 km, the slope is about -1.19; between 700 and 1170 km it is about -0.81 and within 700 km, it is about -0.6. Along solar direction, the slope is -1.05 between 700-1170 km and -0.98 between 1170-5870 km. Along anti-solar direction, it is -0.94 from 940 km to 1880 km; and -1.04 from 3050 km to 5870 km.

Jager: For Jager, the slope is around -0.98 for optocentric distance larger than 1560 km. In a region from 780 km to 1560 km, it is about -1.09 and before 780

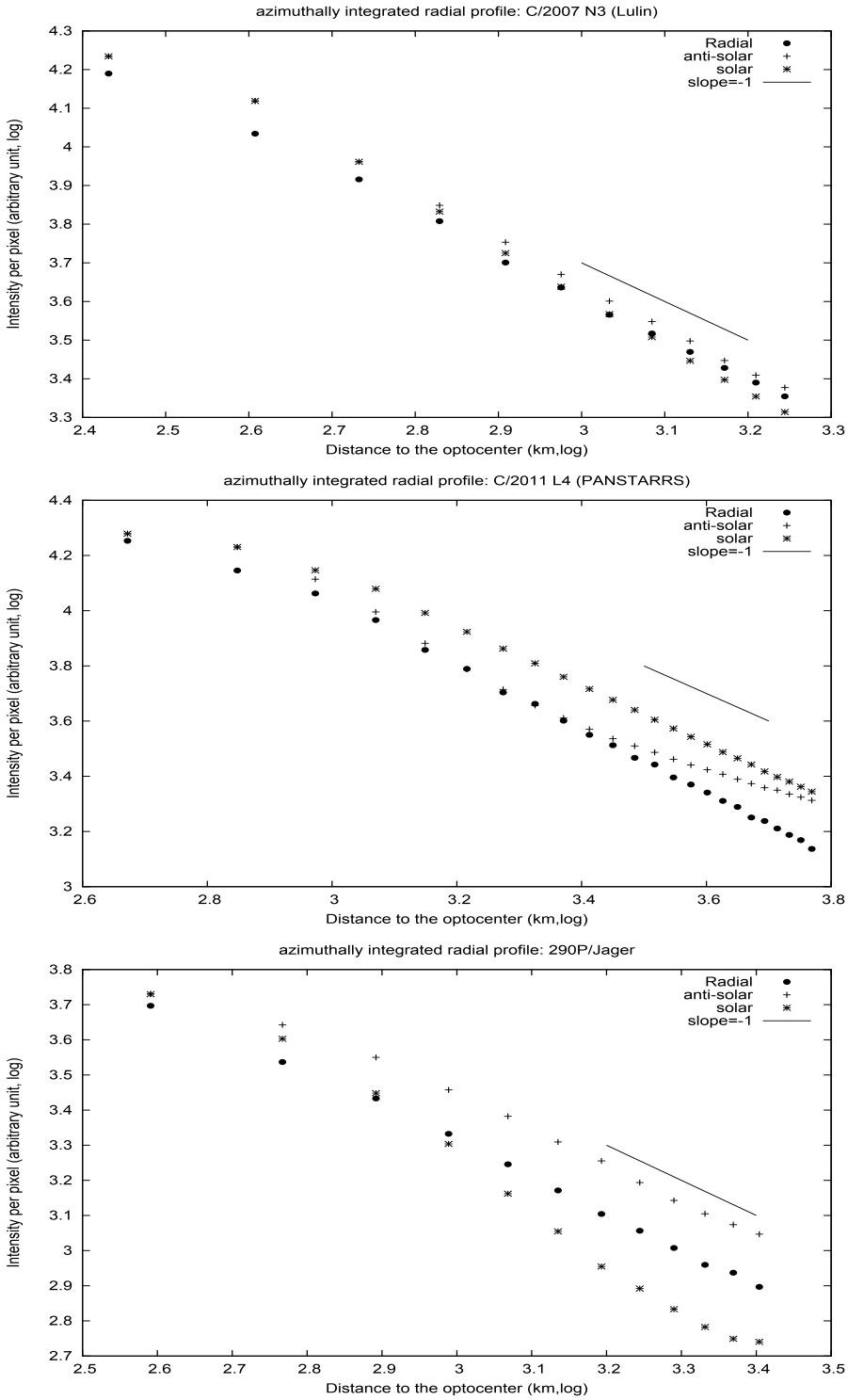

Figure 6.2: Radial, solar, anti-solar profiles of intensity for Lulin, C/2011 L4, Jager.

The azimuthally integrated radial profiles of intensity, along with the profiles of decrease in intensity along solar and anti-solar directions have been obtained as a function of optocentric distance in log-log scale for the three periods of observations. Fit with -1 slope has also been shown.

km, the slope is nearly -0.88. Along the solar direction, the slope changes from -1.64 between 780-1560 km to -1.02 between 1560-2530 km. Along anti-solar direction it is -0.83 between 580-970km and -1.03 between 970-1560km.

Coma morphologies

In this section isophotes, and treated intensity images by a rotational gradient method [Larson and Sekanina, 1984] are presented (Fig. (6.3), (6.4), (6.5)).

Isophotes: The isophotes reveal the shape of the coma in projection on the sky and suggest the presence and position angles of jets. They are here plotted in log scale for intensity.

Garradd: The overall shape of the coma is circular in projection on the sky with a limited sunward-tailward asymmetry. For all observing periods, the main feature is more developed in the projected solar direction. In projection, it extends over more than 40,000 km.

Gehrels: The shape of the coma during Oct, 2011 (i.e. three months before perihelion) was slightly deflected from circularity with an elongation towards the antisolar direction and a structure at about a position angle of 165°. At that period of observation, the comet was at a phase angle of 15.2° and the Sun-comet PA was 72°. After perihelion, during January and February, 2012, the coma is found to be clearly asymmetric, with tailward extension; with the Sun-comet PA being 68° and 71° respectively.

Lulin: Lulin was observed at phase angle 35.7°- 36.7° with solar position angle 277°. The overall shape of coma is about circular with a slight elongation at about PA 190°, which can be consistent with a projected jet perpendicular to the solar direction.

C/2011 L4: The coma of comet C/2011 L4 observed at a phase angle of 38°, is elongated in the antisolar direction; the solar position angle being 130°.

Jager: In case of comet Jager, the coma has a slight extension in the antisolar direction where during observation the solar position angle was 284° and phase angle 14°.

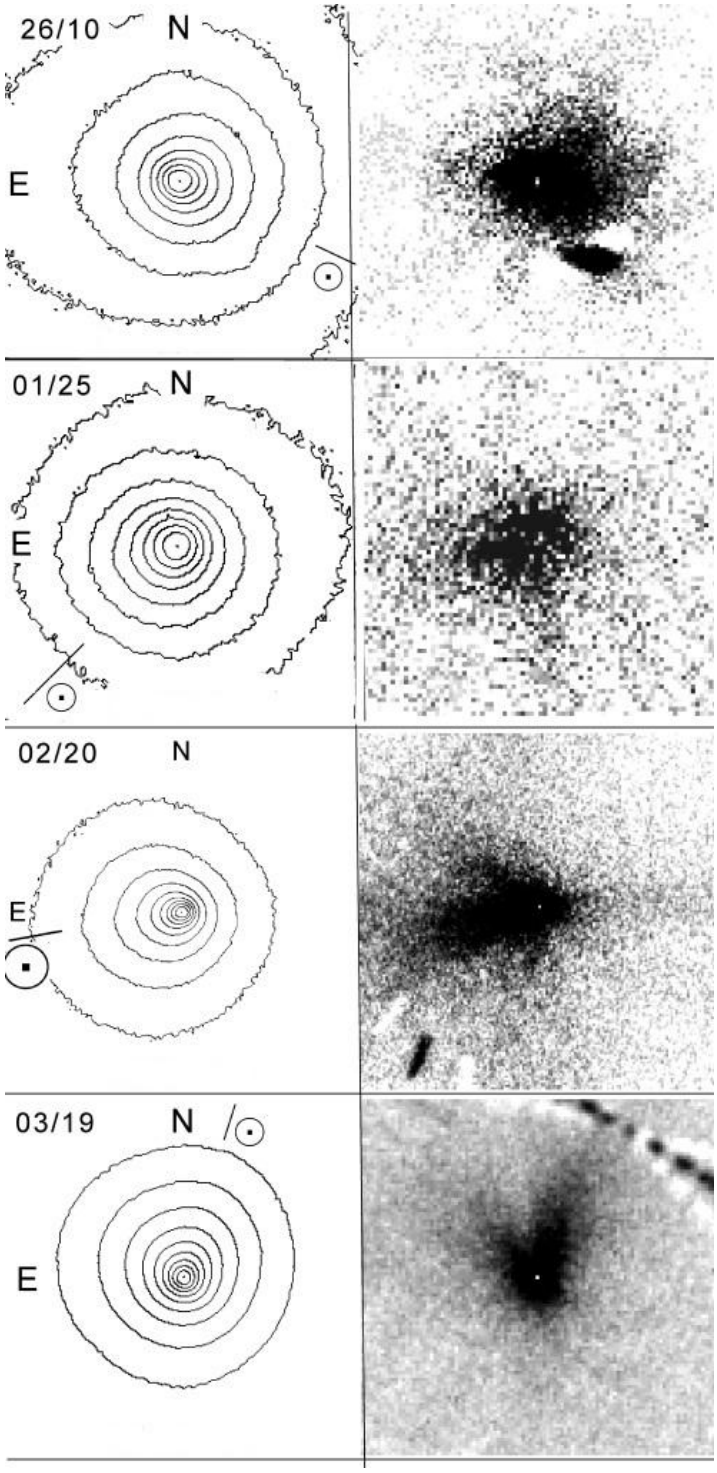

Figure 6.3: Morphologies in intensity for Garradd.
Intensity images for October, January, February, and March. Left column: isophotes with the solar direction indicated by a line with ⊙. Right column: images of intensity treated by a rotational gradient method (in negative). Fields 45,000×45,000 km. North is up and East is left.

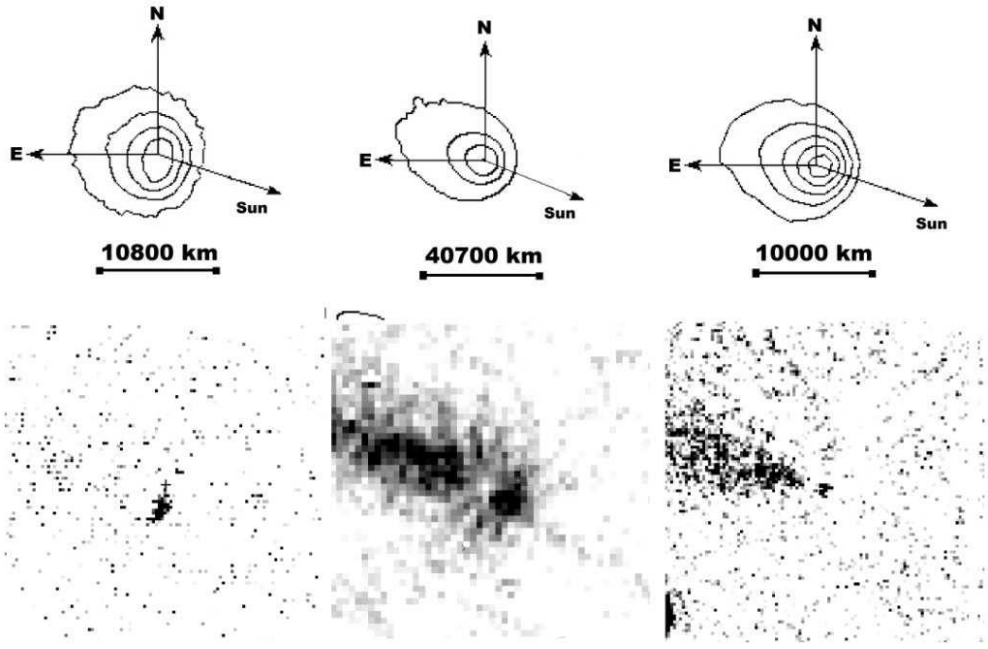

Figure 6.4: Morphologies in intensity for Gehrels.
From left: Oct, 2011; Jan, 2012; Feb, 2012 respectively at phase angle 15.2°, 28.3°, 25.5°. Upper line: Isophotes in log scale. Lower line: Intensity images treated by a rotational gradient method.

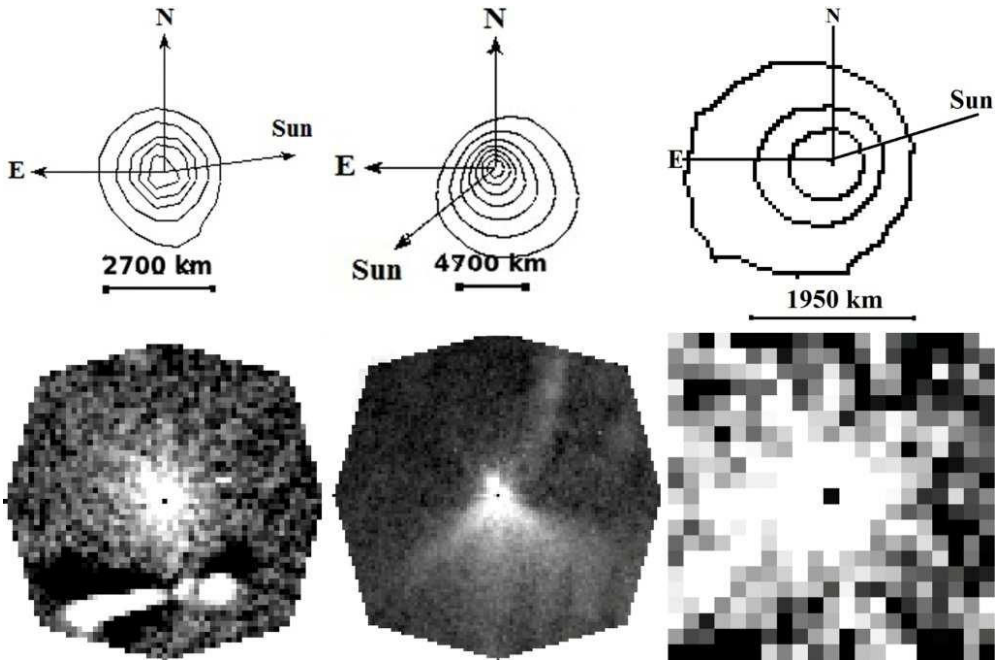

Figure 6.5: Morphologies in intensity for Lulin,C/2011 L4,Jager.
From left- Lulin (17Mar,2009), C/2011 L4 (07May,2013), Jager (27Jan,2014) in R_{OHP} at phase angles 35.7°, 38°, and 14° respectively. Upper line: Isophotes in log scale for intensity. Lower line: Images treated by rotational gradient method.

Treated intensity images: The coma features on CCD images are almost always of low contrast and appear to diminish with increasing distance from nucleus. These features require use of digital image processing techniques to enhance the contrast. Various approaches for image enhancement have been applied to comets (e.g. [Klinglesmith, 1981], [Matuska Jr et al., 1978], [Sekanina and Farrell, 1978], [Wood and Albrecht, 1981]). The most common techniques utilize spatial filtering or take intensity derivatives in some direction. One of the most successful methods has been the radial intensity derivative using radial shift difference algorithm. A shift difference radial to the center of light improves visibility of these features, as it maps the rate of change of emission at a given position angle. A severe limitation is that the features oriented radial to the nucleus, such as jets or ion streamers, do not show. To make these features visible, a rotational shift difference about the optocenter must be applied. The rotational component tends to emphasize features of varying spatial extent depending upon the distance from the nucleus. To ensure that feature of any orientation are retained in the processing, we add two processed images which have the same radial shifts and rotation shifts of the same magnitude but opposite direction. This is known as rotational gradient method [Larson and Sekanina, 1984] which has been applied to the intensity images. The relation between B and B', the brightness of an unprocessed and processed pixel is-

$$B'(x,P;\Delta x,\Delta P) = [B(x,P) - B(x-\Delta x, P-\Delta P)] + [B(x,P) - B(x-\Delta x, P+\Delta P)]$$

where x and P are the point's radial distance and position angle relative to the comet's brightness, $\Delta x, \Delta P$ are the radial and rotational shift.

Garradd: During October, the jets present several fan structures. One fan structure with PA $\approx$ [240°-310°] is close to the solar direction (PA = 244 °) while there is another one in the antisolar direction with PA $\approx$ [50°-130°]. In January, the jets seem to be curved anticlockwise all around the optocenter with a slightly larger extension in the solar direction (PA = 135°). Close to the optocenter three

different ejecting directions are noticed with PA $\approx 110^\circ$, PA $\approx 5^\circ$, and PA $\approx 325^\circ$ (not easily seen on the gray-scale image). During February, structures are well observed in the solar direction with fan-shaped fine jets between PA $\approx [85^\circ 120^\circ]$ (solar PA = 105°) and on the two sides shorter jets at PA $\approx 55^\circ$ and PA $\approx 115^\circ$. Projected on the sky, the main jets extend over more than 22,000 km long. The structures are similar during the three nights of observations through the cometary red and infrared filters. During March observations, a V-shaped structure is observed. Its longer branch is oriented in the solar direction, with an extension of more than 40,000 km at a PA $\approx 340^\circ$. The shortest branch has an extension of more than 12,000 km on the sky with a PA $\approx 35^\circ$. Close to the optocenter the ejection seems to be mainly in the South direction (about antisolar). For the three nights of observation in March, similar structures are observed with all the filters.

Gehrels: In October, 2011 at phase angle 15.2°, three months before perihelion, as on the isophotes a small structure can be noticed at about a position angle of 165°, on the treated intensity image; it is also detected on the isophotes. In the rotational gradient images of January and February, 2012, a distinct structure is observed tailward. The Sun-comet PA during those two periods was 68° and 71° respectively. The structures extensions are about 25000 km in projection on the sky. In January, a sunward relatively short, 7000 km, dust ejection is also observed; it is fainter in February. The appearance and disappearance of structures during the three runs can be explained by varying phase angle, solar position angle and perihelion distance during each run. At low phase angle (15.2°), the dragged materials are about along the line of sight of observer and projected on the same direction on the sky. The direction of ejection of the materials can change with the solar direction PA and with the rotational axis of the nucleus.

Lulin: No prominent structure has been noticed in case of Lulin.

C/2011 L4: A fan-like structure has been noticed between position angles 135°-245° in the treated intensity images of C/2011 L4 corresponding to the enlarged shape of the isophotes in the South direction. Also, three jets on the South direction and two shorter jets in the North direction are noticed.

Jager: In case of Jager, some small structures along the antisolar direction have been detected, which have a correlation to the elongated structures noticed on the isophotes. At low phase angle like 14°, materials ejected along the solar-

antisolar direction are almost in the line of sight of the observer.

6.2.2 Linear polarization:

The variation in polarization values with increase in aperture size is studied first. The polarization maps are obtained thereafter to detect variation in polarization in different regions of coma.

Aperture polarization

To calculate aperture polarization, at first, integrated flux through apertures on each orthonormally polarized component images corresponding to different positions of HWP (for IGO) and polaroid (for OHP) are measured. Then, aperture polarization is obtained from these integrated fluxes using Eq. (5.3) for IGO, Eq. (5.6) for OHP. The polarization through increasing aperture sizes for all the comets under study is presented in Table (6.1)(6.2)(6.3) for the different filters and periods. These polarization values are plotted as a function of phase angle (called phase curve) and discussed in section (6.3.2).

Garradd: The polarization values remain constant when the aperture is sufficiently large before decreasing at the dust coma limit (Table 6.1). This behavior is usually observed in comets. To point out similarities and differences in the dust ejected by comet Garradd and by other comets, the polarization values are compared with observations of other comets. From the available data in the literature, synthetic polarization phase curves were built in different wavelength domains in the visible [Levasseur-Regourd et al., 1996]

Gehrels: For the whole set of observations a decrease of polarization values is observed with increasing aperture (Table 6.2). Nevertheless, this decreasing trend in polarization values with increasing aperture size is within the error bars. For October, systematic lower values of polarization through the red broadband R_{IGO} filter than through the cometary narrow red CR_{IGO} has been noticed. As expected, the polarization value P_r is negative for α= 15.2° and positive for α>25°.

Lulin, C/2011 L4, Jager: For all the three comets, a decrease in polarization values with increasing aperture is observed (Table 6.3). The decrease is prominent in the inner coma region and diminishes at larger aperture called whole coma

Table 6.1: Polarization values P_r (in %) of Garradd for different apertures and wavelengths.

Observatory and period	α°	Filter	5000(km)	10000(km)	20000(km)	30000(km)	40000(km)	θ_r°
IGO								
21 Oct,2011	30.9-30.8	CB_{IGO}	2.6±0.4	2.5±0.5	2.8±0.7	2.3±0.8	NA	-2±10
22 Oct,2011		CR_{IGO}	2.9±0.3	2.8±0.2	2.8±0.6	2.6±0.6	NA	
		CB_{IGO}	2.8±0.5	2.7±0.4	2.3±0.6	2.1±0.8	NA	
		CR_{IGO}	2.7±0.5	2.6±0.4	2.5±0.5	2.5±0.6	NA	
OHP								
26 Oct,2011	30.3	R_{OHP}	2.6±0.5	2.8±0.4	2.8±0.4	2.7±0.4	2.6±0.4	4±10
OHP								
23 Jan,2012	34.8-35.2	R_{OHP}	NA	3.3±0.5	4.1±0.4	4.5±0.5	4.2±0.6	-1±10
24 Jan,2012		CR_{OHP}	NA	4.7±0.2	4.7±0.3	4.2±0.6	4.1±0.6	-15±10
25 Jan,2012		CR_{OHP}	5.7±0.4	4.8±0.3	4.7±0.3	4.3±0.3	3.8±0.5	-5±8
IGO								
18 Feb,2012	34.7-34.3	R_{IGO}	3.6±0.3	3.7±0.3	3.7±0.3	3.7±0.4	3.6±0.5	-2±5
		CR_{IGO}	3.7±0.2	3.6±0.3	3.6±0.3	3.5±0.5	3.3±0.5	9±10
19 Feb,2012		I_{IGO}	3.9±0.2	3.8±0.2	3.6±0.3	3.4±0.4	3.2±0.5	7±10
20 Feb,2012		I_{IGO}	3.8±0.3	3.9±0.2	3.8±0.2	3.7±0.2	3.6±0.5	-2±10
		CR_{IGO}	3.9±0.3	3.7±0.4	3.7±0.4	3.6±0.5	3.5±0.5	
		R_{IGO}	3.9±0.2	3.9±0.3	3.8±0.3	3.8±0.4	3.5±0.5	
		CR_{IGO}	3.9±0.3	3.7±0.4	3.6±0.5	3.7±0.5	3.2±0.6	
OHP								
18 Mar,2012	28.5-28.3	R_{OHP}	2.2±0.3	2.1±0.2	2.2±0.2	2.1±0.1	2.0±0.3	-1±5
19 Mar,2012		CR_{OHP}	2.1±0.3	2.3±0.3	2.2±0.2	2.2±0.3	2.1±0.3	0±3
		CR_{OHP}	2.3±0.3	2.25±0.3	2.3±0.2	2.2±0.2	2.2±0.3	
20 Mar,2012		I_{OHP}	5.0±0.5	3.2±0.2	2.9±0.2	2.8±0.3	2.5±0.3	0±3
		CB_{OHP}	NA	1.9±0.4	2.0±0.4	1.9±0.5	NA	
		CB_{OHP}	NA	2.1±0.4	2.2±0.4	2.0±0.5	NA	
		R_{OHP}	2.3±0.3	2.3±0.2	2.2±0.2	2.1±0.3	2.1±0.3	
		I_{OHP}	4.1±0.4	2.6±0.2	2.4±0.3	2.0±0.3	2.0±0.3	

Table 6.2: Polarization values P_r (in %) of Gehrels for different apertures and wavelengths.

Observatory and period	α°	Filter	2160(km)	4320(km)	7560(km)	10800(km)	15120(km)	20520(km)	θ_r°
IGO									
21 Oct,2011	15.2	CR_{IGO}	-1.2±0.3	-1.1±0.2	-0.7±0.1	-0.8±0.1	-0.8±0.1	-0.8±0.1	93±10
		R_{IGO}	-0.9±0.2	-0.8±0.2	-0.8±0.1	-0.6±0.1	-0.6±0.1	-0.5±0.1	
22 Oct,2011		CR_{IGO}	-0.8±0.4	-0.8±0.3	-0.8±0.2	-0.9±0.1	-0.8±0.1	-0.8±0.1	89±10
				4880(km)	7320(km)	9760(km)	19520(km)	24400(km)	
OHP									
24 Jan,2012	28.3	R_{OHP}		2.4±0.2	2.2±0.2	2.0±0.2	1.6±0.2	1.5±0.3	-3±10
			2000 (km)	4000(km)	7000(km)	10000(km)	15000(km)	20000(km)	
IGO									
19 Feb,2012	25.5	R_{IGO}	1.3±0.3	1.1±0.2	1.1±0.2	1.0±0.2	0.7±0.1	0.6±0.1	4±10
20 Feb,2012			1.1±0.3	1.1±0.2	0.9±0.2	0.7±0.1	0.6±0.1	0.6±0.1	3±10

Table 6.3: Polarization values P_r (in %) of Lulin, C/2011 L4 and Jager for different apertures and wavelengths.

Comet	Date	Filter	1080 (km)	2160 (km)	2980 (km)	4060 (km)	5140 (km)	5410 (km)	θ_r°
C/2007 N3 (Lulin)	17.03.2009	R_{OHP}	5.1±0.3	4.9±0.2	4.7±0.2	4.3±0.2	3.9±0.2	3.9±0.3	5±10
		I_{OHP}	3.3±0.2	4.5±0.2	4.5±0.2	4.3±0.2	4.0±0.3	3.9±0.3	
	18.03.2009	R_{OHP}	3.9±0.2	4.3±0.2	4.3±0.2	4.2±0.2	3.9±0.2	3.8±0.3	-2±10
		I_{OHP}	4.4±0.2	4.3±0.2	4.3±0.2	3.9±0.2	4.0±0.3	4.0±0.3	
	19.03.2009	R_{OHP}	5.4±0.3	5.1±0.2	4.9±0.2	4.5±0.2	3.9±0.3	3.9±0.3	3±10
	20.03.2009	R_{OHP}	5.7±0.4	5.2±0.2	4.7±0.2	4.4±0.2	4.1±0.2	4.0±0.3	-5±10
			2350 (km)	4230 (km)	6110 (km)	7990 (km)	9870 (km)	11750 (km)	
C/2011 L4 (PANSTARRS)	06.05.2013	R_{OHP}	5.9±0.3	5.9±0.3	5.8±0.3	5.7±0.3	5.6±0.4	5.5±0.4	-1±10
	07.05.2013	R_{OHP}	6.5±0.4	6.1±0.3	5.9±0.3	5.8±0.3	5.6±0.4	5.5±0.4	10±10
		I_{OHP}	6±0.3	5.4±0.3	5.2±0.4	5.1±0.4	star	star	
			780 (km)	1170 (km)	1560 (km)	2340 (km)	3120 (km)	3900 (km)	
290P/Jager	27.01.2014	R_{OHP}	-7.3±0.5	-6.8±0.3	-5.4±0.2	-3.6±0.2	-2.4±0.2	-1.6±0.2	98±10
	28.01.2014	I_{OHP}	-6.2±0.4	-5.4±0.2	-5.0±0.2	-2.9±0.2	-1.9±0.2	-1.7±0.2	

polarization. Considering the error bars, the whole coma polarization values are nearly similar for the two filters- R_{OHP}, I_{OHP} and for the different nights, except in the inner coma where variations are distinct.

Polarization maps

Polarization maps are obtained by processing the four polarization component images of a particular set as a whole, using Eqs. (5.3) and (5.6). The variation of θ_r through coma being insignificant, the polarization values do not change sign on the polarization map. The polarization map of Garradd is shown in Fig. 6.6, for Gehrels in Fig.6.7 and for other three comets (Lulin, C/2011 L4, Jager) is shown in Fig.6.8. All maps are in red wavelength.

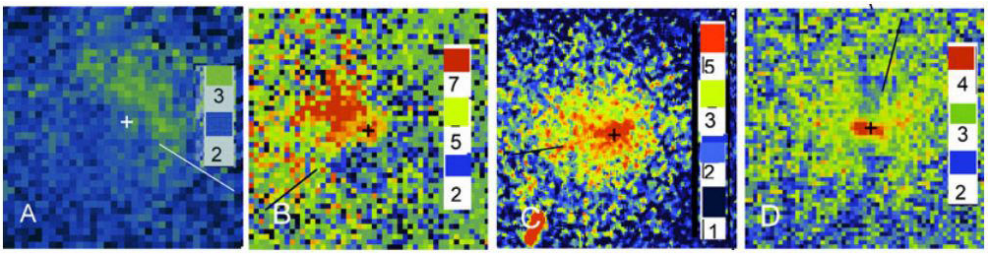

Figure 6.6: Polarization map of Garradd.
Polarization maps: A) 2011 October (R_{OHP} filter), B) 2012 January (CR_{OHP} filter), C) February (R_{IGO} filter), D) March (I_{OHP} filter) observations. To improve the display a Gaussian filter was applied. Optocenter +, straight line: solar direction. Color or gray scales in percent. Field is 45,000×45,000 km. North is up and East is left. Some images have been treated by a median filter.

Garradd: Polarization maps for the four periods of Garradd are presented in Fig. (6.6). The different regions have polarization values different only by about 1%, which is at the limit of the error bars. In October, the central region presents a polarization of ≈ 2.6% and increases slightly in the NorthWest direction shaping an extending arc structure (Sun is about South-West) with a polarization of ≈ 3%. The difference is small but this structure is observed in different images and seems to be real. In January, the higher polarization region extends NorthEast from PA ≈ 20° to PA ≈ 120°, close to the solar direction. The maximum polarization value is about 6% while in the South-West opposite direction it is about 4%. In February,

the central region presents a polarization value between 3% and 5% at the center. It extends on average up to 7000 km distance. The polarization in the surrounding region has an apparent width around the central region of about 12,000 km with a value of approximately 3% and decreases farther away. Whenever jets appear on the treated intensity image (East direction), they are also present on the polarization map with approximately 4% polarization (the surrounding polarization being 3%). Their extension is greater than 20,000 km. In March, the central regionwith an average polarization of about 4%is elongated (EastWest) with an extension of 9000 km and a width of 4000 km. Farther away a symmetric 'butterfly' shape is observable on both sides extending over 14,000 km with an average polarization value of 3%. In the outer coma, the polarization value falls down to 1%. The butterfly wings extend further towards the Sun.

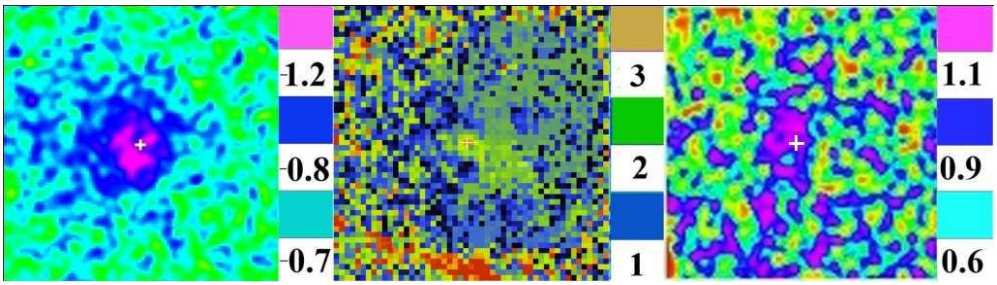

Figure 6.7: Polarization map of Gehrels.
From left: Oct, 2011; Jan, 2012; Feb, 2012 respectively at phase angle 15.2°, 28.3°, 25.5°. Polarization values are in %. The field of views, the North, East and the solar directions are same as on Fig (6.4)

Gehrels: For October, the difference in polarization noticed on the polarization map along the observed structure at 165° is within the limit of error. But the polarization is slightly more negative around the optocenter, though the expected deep polarization is not observed. For January, on the polarization map, an eventual slightly greater polarization in the sunward direction can be observed. For February, on the polarization maps there is no difference of polarization along the tailward structure that appeared on the treated intensity image and surrounding coma.

Lulin: For Lulin, higher polarization is noticed surrounding the central coma, which decreases gradually.

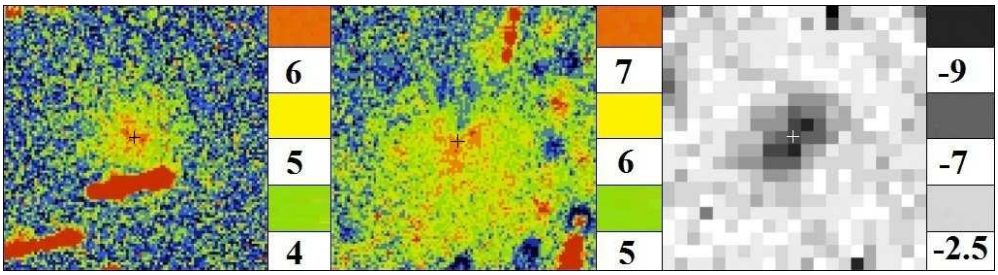

Figure 6.8: Polarization map of Lulin, C/2011 L4, Jager.
From left- Lulin (17.03.2009), C/2011 L4 (07.05.2013), Jager (27.01.2014) in R_{OHP} at phase angles 35.7°, 38°,14° respectively. Polarization values are in %. Field of view for Lulin 13700x13700 km^2, for C/2011 L4 24000 x24000 km^2, for Jager 4100x4100 km^2. N, E and solar directions are same as in Fig (6.5).

C/2011 L4: In case of C/2011 L4, a correlated higher polarization along the observed structures (on the rotational gradient image) is noticed on the polarization map.

Jager: A deep negative polarization around central coma of Jager has been observed on its polarization map. Also, the polarization value decreases progressively with optocentric distance.

6.3 Discussions on present set of results

6.3.1 Intensity variations in the coma:

For the analysis of the overall aspect of the coma, azimuthally integrated radial intensity profiles (1-D surface brightness profiles) have been obtained from the images. The -1 slope of the log-log profiles of intensity decrease with aperture radius indicates an isotropic coma if the sky background is subtracted properly. When the effect of solar radiation pressure becomes important, the profiles can be as steep as -1.5 [Jewitt and Meech, 1987]. Steeper profiles (slope greater than -1 in magnitude) may be caused by non-steady state emission, or by fading grains, whereas shallower profiles (slope smaller than -1 in magnitude) require a source function in the coma (e.g., fragmenting grains or production of gas from grains). For solar and anti-solar profiles, a steeper slope indicates that dust is moving away

from the region; and a shallower slope indicates that dust is replenishing the region. In the present work, the azimuthally integrated radial intensity profiles, it is noted that the slope of intensity decrease is nominal (slope -1) at large optocentric distances for all the periods of observation. The log-log profiles of intensity decrease between solar and anti-solar direction for all periods of observation indicate a higher intensity along the solar direction. The slope is found to increase (in magnitude) progressively with the optocentric distance in the solar direction and that along antisolar direction is found to decrease (in magnitude) for all periods. So, it is understandable that the dusts are driven towards the anti-solar direction by solar radiation.

Garradd: New and periodic comets have both been observed by imaging polarimetry at low or intermediate phase angles. High-P_{max} comets present generally well structured jets with a higher polarization than the surrounding coma and extending at relatively large distances from their nucleus as compared with the coma size. The presence of submicron-sized grains, in highly porous large aggregates, has been suggested in the jets and arcs of comet Hale-Bopp ([Hanner et al., 1997], [Hayward et al., 2000], [Hadamcik and Levasseur-Regourd, 2003b]). More generally, the particles in the jets of high-P_{max} comets seem to be made of similar grains and structures but the number of the jets is relatively smaller. In the coma of low-P_{max} comets, structures may be absent on the polarization maps, e.g., in comet C/1989 X1 Austin [Eaton et al., 1992] or high polarization regions with small extension around the optocenter may be found. In that case, the ejected dust probably consists of large dark particles, moving slowly and eventually breaking down. This seemed to be the case for comet 9P/Tempel 1 before the Deep Impact event and comet 67P/Churyumov-Gerasimenko before perihelion ([Hadamcik et al., 2007a], [Hadamcik et al., 2010]). The jets in comet Garradd are preferentially oriented in the solar direction.

78P/Gehrels: A solar-antisolar asymmetry is confirmed from the contours of the intensity images. From the intensity images treated by rotation gradient method, an ejection of materials along antisolar direction is apparent in case of January and February, 2012 observations at a phase angle 28.3° and 25.5° respectively. But there is no indication of such distinct structures in October, 2011 images. Only a small structure can be noticed there. Amongst the three sets of

observations, the least distance (1.21 au) of the comet from Earth was in October. But at that time, comet's distance from Sun was largest (2.12 au) and the phase angle was lowest (15.2°). At such small phase angles the ejected materials along the solar-antisolar direction are almost in the line of sight to the observer. This fact, together with the largest solar distance of the comet might have caused an apparent suppression of structures along solar-antisolar direction during October, 2011.

Lulin, C/2011 L4 and Jager: For Lulin and Jager, the slope of decrease of radial profile is about -1 (-1 for Lulin, -0.98 for Jager) at large optocentric distances. The slopes of Jager along solar (-1.64) and anti-solar (-0.83) direction clearly indicate that the dusts are pushed tailwards. For C/2011 L4, the slope is about -1 (solar -1.05,-0.97; anti-solar -1.04, -0.94) along solar and anti-solar direction. And its radial slope (-1.18) is slightly higher (in magnitude) than -1 at outer coma; meaning that the dusts are not isotropically distributed on average. This is an indication for the presence of jets.

6.3.2 Polarization phase curve:

Polarization values as a function of phase angle are characteristic of average physical properties of cometary dust. In Fig. (6.9), (6.10) and (6.11), the polarization values reported in Table (6.1), (6.2) and (6.3) are plotted as a function of phase angle and are compared to the polarimetric phase curves of so-called 'high-P_{max} comets' and 'low-P_{max} comets' ([Levasseur-Regourd et al., 1999], [Hadamcik and Levasseur-Regourd, 2003c]). From the tables mentioned, data with sufficiently large apertures are chosen for plotting to cover the polarization of whole coma.

Three classes of comets have been defined based on the maximum polarization value and more generally the positive branch on the polarimetric phase curve. These are: (1) 'low-P_{max} comets': with a low maximum polarization $(18 \pm 3)\%$, (2) 'high- P_{max} comets': with a higher maximum polarization $(27 \pm 3)\%$, and (3) 'Hale-Bopp group of comets': with a positive polarization higher than all other comets (although only observed up to α=48°) ([Levasseur-Regourd et al., 1996], [Hadamcik and Levasseur-Regourd, 2003c], [Hadamcik and Levasseur-Regourd, 2003b]).

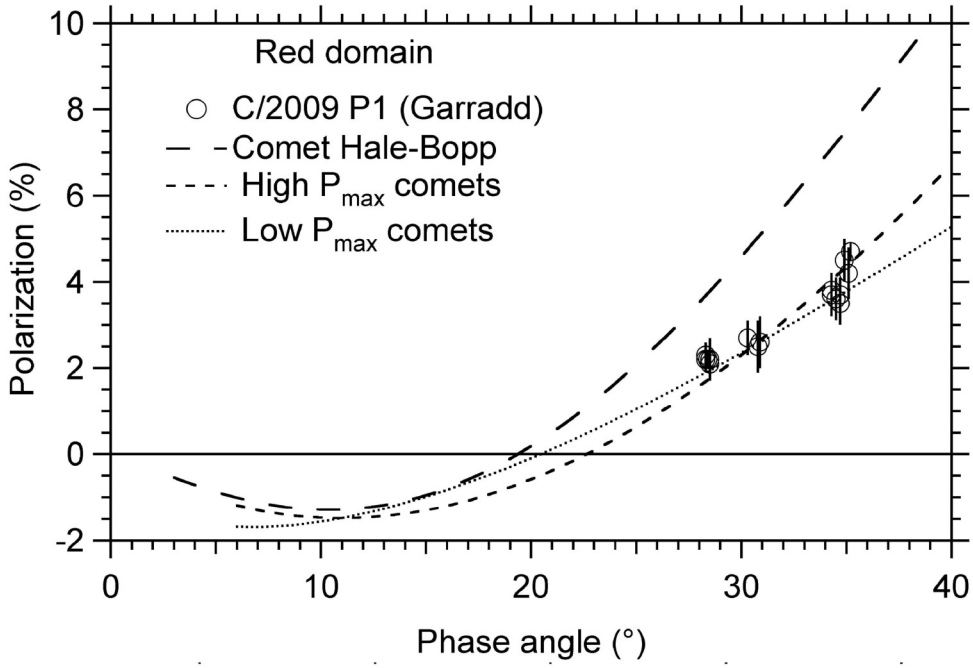

Figure 6.9: Fitting whole coma polarization values of comet Garradd with the synthetic phase curves.

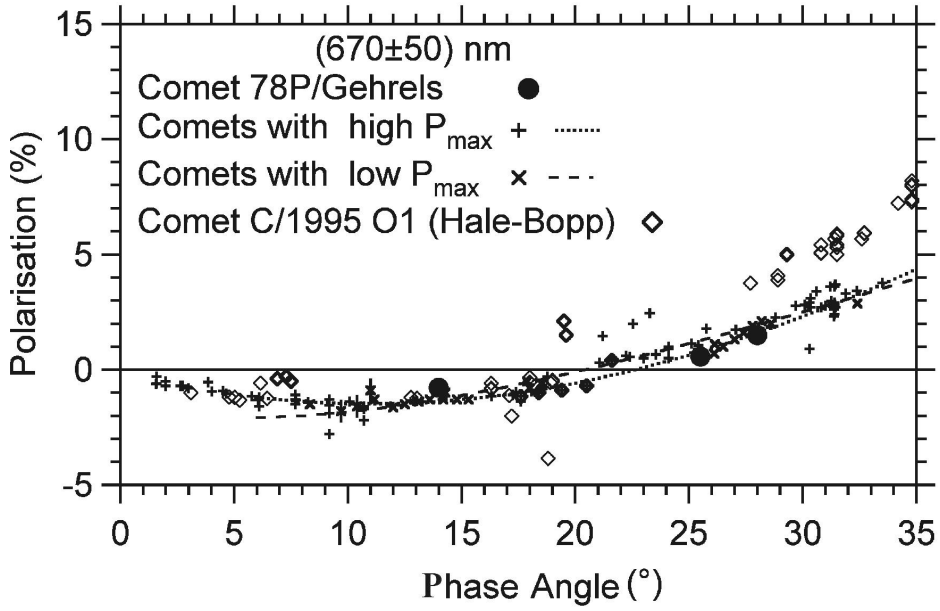

Figure 6.10: Fitting whole coma polarization values of comet Gehrels with the synthetic phase curves.

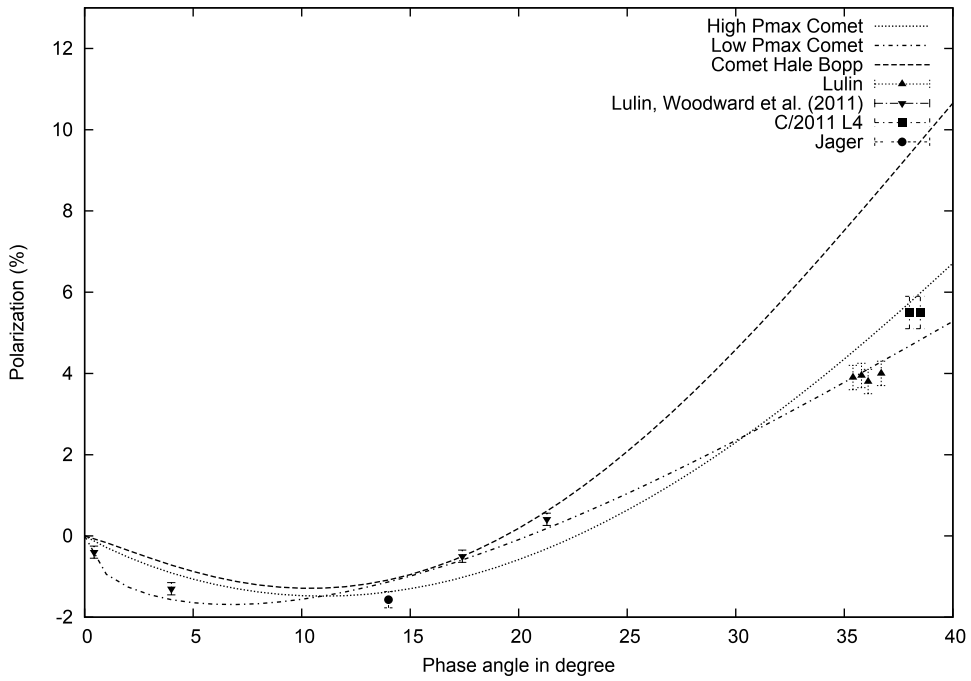

Figure 6.11: Fitting whole coma polarization values of comets Lulin, C/2011 L4, Jager with the synthetic phase curves.
Polarization values obtained by Woodward et al. 2011 have also been used for comparison.

Classification of comets into different classes based on the synthetic phase curves ([Levasseur-Regourd et al., 1996], [Hadamcik and Levasseur-Regourd, 2003c]) is generally possible if the polarization data are available for large phase angles greater than 35°. To fit all the data of comets to the three classes of comets, an empiric trigonometric function proposed by [Lumme and Muinonen, 1993] has been used (as already mentioned in section (4.3.3)-

$$P = b[\sin\alpha]^{c1}[\cos(\alpha/2)]^{c2}\sin(\alpha - \alpha_0) \tag{6.1}$$

The origin of this difference in polarization value shown by different group of comets is yet not understood completely. For example, [Kolokolova and Kimura, 2010b] had suggested slowly moving large and compact particles for low-P_{max} comets and submicron-sized grains in fluffy aggregates for high-P_{max} comets. Such different kinds of particles are sometimes found in the same comet at different orbital epochs [Hadamcik et al., 2010]. It is noted that the phase angle and slope at inversion seem to be slightly higher for high-P_{max} comets than the low-P_{max} ones [Levasseur-Regourd et al., 1996].

Garradd: The classification is generally possible once measurements are available at phase angles larger than 35°. The results for comet Garradd are similar to those obtained for other comets (Fig. 6.9), perhaps closer to the high-P_{max} comets class (but the difference between high and low-P_{max} comets is small at phase angles smaller than 35°). [Bodewits et al., 2012] suggested similarities between comet Garradd and comet Hale-Bopp. The polarization values of comet Hale-Bopp are much higher than those obtained for any other comets [Levasseur-Regourd et al., 1999], including presently studied comet Garradd indicating at least different physical properties for their dust.

Gehrels: At low phase angles (lower than 35°), the synthetic phase curves are very close to one another. Our observation of Gehrels is below 29°. Thus it is difficult to classify Gehrels from the present observations. But at similar low phase angle comet Hale-Bopp showed higher polarization due to numerous submicron-sized grains present in it. So, it is just confirmed that Gehrels is not similar to comet Hale-Bopp. The use of narrowband filters is to isolate the light emitted by various molecular species and reflected solar radiation by dust grains

in cometary coma [Schmidt and van Woerden, 1957]. For October, the systematic lower values of polarization through the red broadband R_{IGO} filter than through the cometary narrow red CR_{IGO} filter may be attributed to contaminations by emission lines of the gaseous species but the difference is smaller than the error bars. A good correlation of polarization values with the synthetic phase curve in the in the positive branch indicates that the contamination is small.

Lulin, C/2011 L4 and Jager: Considering the error limits, the whole coma polarization values of Lulin, observed between 35-36° phase angle, seem to lie close to low-P_{max} class of comets. [Woodward et al., 2011] observed the comet below 22°; their data are also plotted on the graph. Though at that phase angle the synthetic phase curves are very close to one another, yet it appears closer to low-P_{max} class within the error limits. Polarization values of C/2011 L4, observed at 39° phase angle seems to be closer to high-P_{max} class of comets. Jager was observed below inversion angle and as expected, low negative whole coma polarization is found.

6.3.3 Polarization maps:

Garradd: On the polarization maps, jets are mainly observable in January, February, and in March. Their extension is more than 20,000 km. Their properties are consistent with a population of submicron to micron-sized grains in aggregates. In January and February the higher polarization and extension of the jets may be the result of an increase in activity after perihelion. On March maps, the higher polarization region is relatively restricted but the butterfly-shaped structure may be the result of particles breaking up after leaving the central high polarization region. Such behavior has been observed, e.g., around the main fragment of comet C/1999 S4 (LINEAR) during its complete disintegration [Hadamcik and Levasseur-Regourd, 2003a].

Gehrels: The jet-like structures, observed in high-P_{max} comets, have usually a higher polarization than the surrounding coma and are well collimated. In low-P_{max} comets some high polarization regions may exist but their extension is often limited to regions close to the nucleus. In case of Gehrels, on the polarization map of all the epochs, no significant difference in polarization values is noticed along

the tailward structures and the surrounding coma. The only higher polarization region is observed just after perihelion in the solar direction in January. There are some past observations where enhanced gradient region did not present any polarimetric difference with the surroundings. For example at α= 18°, the tailward structure (on the intensity image) of comet 22P/Kopff, had the same polarization as the background [Hadamcik and Levasseur-Regourd, 2003c]. At α= 6.9°, for comet C/1995 O1 (Hale-Bopp), the perpendicular large structure to the solar direction has the same polarization as the background, out of five jets detected around the optocenter [Hadamcik and Levasseur-Regourd, 2003c]. The absence of difference in polarization suggests similar properties of the particles along the structures and surrounding coma.

Lulin, C/2011 L4 and Jager: Higher polarization noticed surrounding the central coma of Lulin decreases gradually with radial distance from nucleus. In most of the cases; low-P_{max} comets show some high polarizations, limited to regions close to the nucleus ([Kiselev et al., 2005], [Hadamcik et al., 2007a]). In high-P_{max} comets, jet activity is more important and the jets extend far from the nucleus ([Hadamcik and Levasseur-Regourd, 2003b], [Hadamcik et al., 2013]). The structures noticed in case of C/2011 L4 have a higher polarization than the surrounding coma and are correlated to jets, confirming the classification of the comets into the high-P_{max} class. In some comets with an important seasonal effect such as comet 67P/Churyumov-Gerasimenko, jets can be observed in low-P_{max} comets depending of the epoch of observations [Hadamcik et al., 2010]. The deep negative polarization around central coma of Jager is called polarimetric halo. Such central polarimetric halo was observed in different comets [Hadamcik and Levasseur-Regourd, 2003c]. Different compositions were suggested for this region but it is not yet resolved. The polarization is less negative, when the distance from the center increases. Higher polarization is detected along the observed jets. Comets belonging to the low-P_{max} class sometimes present less activity than high-P_{max} ones. For example, CCD images of comet C/1989 X1 (Austin) do not present any jet structure [Eaton et al., 1992]. Some other low-P_{max} comets present a high polarization near the nucleus and an important decrease of polarization as a function of aperture size in this region, e.g. 23P/Brorsen-Metcalf [Chernova et al., 1993] or 2P/Encke [Jockers et al., 2005]. Nevertheless for this last comet, a lower

polarization in the inner coma was found by [Jewitt, 2004] for some other epoch. This inner coma polarization difference is discussed in [Hadamcik and Levasseur-Regourd, 2009]. [Kolokolova and Kimura, 2010b] suggested slowly moving large and compact particles for low-P_{max} comets and submicron-sized grains in fluffy aggregates for high-P_{max} comets.

6.4 Comparative study with other results

Garradd: The comet was studied by both ground-based observations [Villanueva et al., 2012] and space-based observations from, e.g., Swift satellite and Deep Impact space probe [Bodewits et al., 2012]. Both have indicated a large dust production rate, even far away from the Sun, suggesting that its activity might not only be triggered by water ice sublimation. Bodewits reported Swifts UVOT observations of the comet at regular intervals at heliocentric distances between 3.5 and 1.7 au on its inbound trajectory and found that its behaviour is nearly similar to the behaviour of comet Hale-Bopp at comparable heliocentric distances. Cometary dusts are dragged into the low-density gaseous coma by sublimating ices. This is efficiently studied by observations of solar scattered light and specifically for its partial linear polarization (e.g., [Dollfus et al., 1988], [Levasseur-Regourd et al., 1999], [Hadamcik and Levasseur-Regourd, 2003c]). Linear polarization measurements of the light scattered by dust on comet Garradd have also been performed by [Kiselev et al., 2012], between August 2011 and February 2012 at phase angles of about 13°, 15°, 22°, 30°, 31°, 32°, and 37°. Das et al. 2015 reported polarimetric study of comet Garradd, observed for three nights in March and May, 2012 at the phase angles 28°.2, 28°.1 and 21°.6. The polarization value obtained by them, observed at α = 28°.1 is about 2% for λ = 0.684 μm, but at such phase angle and wavelength the polarization value for the comet Hale-Bopp is $\sim$ 4 % [Manset and Bastien, 2000]. Jet activity observed in the treated intensity image of 2012 March, seems to be absent in the 2012 May observation. The polarimetric results of both the authors perfectly agree with our results and complement them. Comet Garradd does not show any resemblance with comet Hale-Bopp at such phase angle. The dusty coma shows a high degree of linear polarization, but not as high as the comet Hale-Bopp. This contradicts the result with [Bodewits et al., 2012].

Gehrels: [A'Hearn et al., 1995] from one observation at a heliocentric distance of 2.36 au after perihelion, had classified the comet as carbon-chain depleted. [Fink and Hicks, 1996] observed the comet on October 9, 1989, at a heliocentric distance of 2.35 au and obtained a spectrum which seems to be missing of notable gaseous emissions. [Lowry and Weissman, 2003] observed it on May 24, 2001, at a heliocentric distance of 5.5 au before perihelion; the comet was active and its nucleus radius was estimated to be 1.41$\pm$0.12 km if an albedo of 0.04 was assumed. [Snodgrass et al., 2008] observed the comet on March 2, 2006, at a heliocentric distance of 3.84 au after perihelion; the comet was active. epifani2011dust with a multicolor UBVRI broadband photometry observed the comet on October 27, 2004, at a heliocentric distance of 2 au, some days after perihelion and close to the Earth. The comet was bright and showed a well-developed coma with a tail-like structure and an important solar, antisolar asymmetry. A surface brightness slope was deduced and found to be -1.54$\pm$0.02. Some axisymmetric lobes were detected on treated images (red and infrared filters) but it was difficult to interpret further.

Through the post-perihelion observations in 2004, [Epifani and Palumbo, 2011], observed similar coma shape with an important solar-antisolar asymmetry. The slopes of decrease in intensity with increasing aperture radius are deeper at this epoch but the conclusions are similar with an important effect of solar radiation pressure and a well-defined tailward feature in the treated intensity images. The ejection in the solar direction seems to be more important and more extended in January, 2012. The higher polarization in the jets indicates that freshly ejected particles are slightly different from background particles. For those pushed in the tailward direction, the higher polarization is no more observed. Some of the particles can loss some carbonaceous compounds or be fragmented, but the snapshot observations do not allow to interpret the difference further.

According to [Epifani and Palumbo, 2011], and their Afρ determination, comet Gehrels is a very dusty comet. Afρ is a proxy of dust activity with 'A' the grain albedo, 'f' the filling factor in the aperture and 'ρ' the linear aperture in cm [Ahearn et al., 1984]. This is compatible with the absence of emission lines [Fink and Hicks, 1996]. The absence of well-focused jets suggests a low-P_{max} comet but this classification is not straightforward for phase angles smaller

than 35°. It is interesting to note that a dusty comet is generally considered as a high-P_{max} ([Chernova et al., 1993], [Kolokolova and Kimura, 2010a]).

The red color of the dust, found by [Epifani and Palumbo, 2011], are in favor of large particles in the coma and particles made of, or covered by carbonaceous compounds as suggested by experiments on analogs ([Hadamcik et al., 2007a], [Hadamcik et al., 2007b]). The polarization measurements suggest that jets with submicron-sized aggregates such as found in well-focused jets of high-P_{max} comets or Hale-Bopp, are not ejected at the time of these observations. Nevertheless, the particles being very sensitive to the solar radiation seem to be porous.

Lulin: The concerned comet is a poorly studied one. [Woodward et al., 2011] found that comet C/2007 N3 (Lulin) shows the typical negative polarization in both optical (R=0.676 μm) and near-infrared (H=1.65 μm) at low phase angles (0.44° to 21°). Though it is not justified to comment on class of comet below 35, but, considering the error limit, polarization values of Lulin calculated by them seem to lie closer to low-P_{max} class of comets like our results. They concluded that the dust in comet C/2007 N3 (Lulin) is dominated by large and compact aggregate particles, made up of thousands of small monomers.

C/2011 L4: An analysis of the photometric data of Oort-cloud Comet C/2011 L4 (PANSTARRS) observed in May-June 2012 at heliocentric distance of 4.4-4.2 au is presented by [Ivanova et al., 2014]. Their estimations of the relative dust production rate of the comet show high activity level of the comet at heliocentric distant beyond 4 au as well. These results for the Comet C/2011 L4 (PANSTARRS) support the idea that long-period comet are more active along the entire orbit and especially at large heliocentric distance [Meech, 1988]. Yang and group did multi-wavelength observation on the comet and reported detection very fine water ice grains in the coma of C/2011 L4. They also concluded that C/2011 L4 is an unusually dust-rich comet with a dust-to-gas mass ratio > 4 [Yang et al., 2014].

Jager: Carbon dioxide is one of the most abundant ices present in comets and is therefore important for understanding cometary composition and activity. According to [McKay et al., 2016], the CO_2/H_2O ratios derived from the Spitzer images for Jager is 31.3$\pm$4.2 $\%$ (derived under the assumption that con-

tamination from CO emission is negligible). The CO_2 abundance measured is significantly larger than the average abundance comets at similar heliocentric distance (2.18 au). [Roy et al., 2015] reported the polarimetric observations of comet 290P/Jager, before perihelion passage (December, 2013) and just after their perihelion passage (April, 2014). The deviation of the brightness profile in the solar and antisolar direction from the standard canonical nature confirms the time variation in dust outflow which is mainly due to the modulation of dust production rate, sublimation of high albedo icy grains due to the solar radiation pressure and variation in the physical properties of dust. The degree of polarization is found to be -1.6$\pm$0.3 $\%$ at 13° phase angle; and +2.5$\pm$0.5 $\%$ at 27° phase angle. It has been noticed from polarization maps that the polarization is highly negative in the circumnucleus halo of comet 290P/Jager during December observation, while a high positive polarization is being observed at the near nucleus region of both the comets in April observation. The polarization values and detection of halo are consistent with our results.

6.5 Conclusion

Five comets (viz C/2009 P1 Garradd, 78P/Gehrels 2, C/2007 N3 (Lulin), C/2011 L4 (PANSTARRS), 290P/Jager) appearing close to Earth between 2009-2014 were observed and studied by some Indian and French astronomers, in a joint campaign under CEFIPRA (Indo French Centre for the Promotion of Advanced Research) funded project. They were observed with the 2m telescope at IUCAA Girawali Observatory (IGO) in India and the 0.8 m telescope at Haute-Provence Observatory (OHP) in France. All the observations were made by imaging polarimetry method, at low phase angles ($<$40°), in the red and near infra-red wavelength domains. Both broadband and to avoid gaseous contaminations, narrowband cometary filters were used.

Comets C/2009 P1 (Garradd) and 78P/Gehrels 2 were observed from IGO and OHP between October 2011 and March 2012. Comet C/2009 P1 Garradd was observed during five observational runs when its phase angle varied between 28° and 35°. Comet 78P/Gehrels 2 was observed during three observational runs; between phase angle 15.2° to 28.3°. Other comets were observed between 2009

and 2014 from OHP. These are - i) C/2007 N3 (Lulin), observed during 17-20 March, 2009; at a phase angle between 35.7- 36.7°, ii) C/2011 L4 (PANSTARRS), observed on 6 & 7 May 2013; at a phase angle 38-39°, iii) 290P/Jager, observed on 27 & 28 January 2014; at a phase angle 14-15°.

In conclusion, for Garradd, the polarization phase curve indicates that the linear polarization of the scattered light by the dust particles is similar to those of other comets. Jet activity is observed on each period. After perihelion, in January, February, and March, higher polarization jets are apparent in the solar direction. This activity seems to confirm a classification among the high-P_{max} class of comets with ejection of small submicron to micron-sized grains. In case of Gehrels, from the polarization phase curve, it is evident that the positive branch of the comet is below that of the very active comet Hale-Bopp, but at such low phase angles it is difficult to conclude between low-P_{max} and high-P_{max} class of comets to which it belongs. From the polarization map it is confirmed that, after perihelion, in January and February, the observed intensity structures along the tailward direction have similar properties than the background coma. The particles ejected in the solar direction in January seem to be relatively large and with a low number density, but this structure was no more observable in February, 2012. The nonexistence of important jet activity suggests a possibility for 78P/Gehrels to be a member of the low-P_{max} class of comets. The phase curve of Lulin indicates the possibility of it to be a low-P_{max} type of comet, also no activity has been detected. In case of C/2011 L4, some jet structures, along north and south having a polarization higher than the surrounding coma have been noticed. This, along with phase curve confirms C/2011 L4 to be a high-P_{max} type of comet. Like 81P/Wild2, 22P/Kopff; the deep negative polarization around central coma called polarimetric halo is noticed in case of 290P/Jager. A small jet is also detected along anti-solar direction.

In the present work, we have studied two Jupiter Family comets and three non-periodic Oort cloud comets. This will help to understand the taxonomy and evolution of Oort family and Jupiter class comets. Our work is a contribution towards knowing the comets better, and also towards understanding the evolution of solar system.